Published in final edited form as:
Nanoscale. 2013 January 7; 5(1): 143–146. doi:10.1039/c2nr31877f.

Surface chemistry-mediated penetration and gold nanorod thermotherapy in multicellular tumor spheroids†

Shubin Jin[a,⊥], **Xiaowei Ma**[a,⊥], **Huili Ma**[a], **Kaiyuan Zheng**[a], **Juan Liu**[a], **Shuai Hou**[b], **Jie Meng**[a], **Paul C. Wang**[c], **Xiaochun Wu**[b,*], and **Xing-Jie Liang**[a,*]

[a]Laboratory of Nanomedicine and Nanosafety, Division of Nanomedicine and Nanobiology, National Center for Nanoscience and Technology, China, and CAS Key Laboratory for Biomedical Effects of Nanomaterials and Nanosafety, Chinese Academy of Sciences, Beijing 100190, P. R. China

[b]CAS Key Laboratory of Standardization and Measurement for Nanotechnology, National Center for Nanoscience and Technology, Beijing 100190, P. R. China

[c]Laboratory of Molecular Imaging, Department of Radiology, Howard University, Washington, D.C. 20060, United States

Abstract

We investigated the penetration and thermotherapy efficiency of different surface coated gold nanorods (Au NRs) in multicellular tumor spheroids. The current data show that negatively charged Au NRs, other than positively charged Au NRs, can penetrate deep into the tumor spheroids and achieve a significant thermal therapeutic benefit.

Gold nanorods (Au NRs) are well-developed nanomaterials that have various applications in biomedical research, such as cell imaging, drug and gene delivery and thermal therapy, because of their biocompatibility and unique optical properties.[1–4] In thermal therapy, the localized surface plasmon resonance (LSPR) effect enables Au NRs to convert luminous energy into heat when activated by laser at a specific wavelength.[5] The LSPR maximum can be tuned to the near-infrared (NIR, 700–900 nm)[6] region by controlling the aspect ratio and size of the Au NRs.[7] Thus, the laser powerfully penetrates through human tissues and can reach deep sites in the lesions. Additionally, it is harmless to cells without Au NRs.[4, 8]

The bio-distribution of Au NRs in tumor tissues is still unclear. Most tumor cells, unlike normal tissue cells, are not reached by vasculature: blood and lymphatic vessels.[9] Many effective *in vitro* drugs fail to be used in clinical settings because of the poor distribution at the tumor site; therefore, they could only achieve an effective concentration in the cells close to the vasculatures.[9] The ability of Au NRs to penetrate the tumor tissues and accumulate at sites distant to the blood vessels is essential for the success of the thermal therapy.

Previous studies have reported that the surface chemistry is a key factor affecting the cellular uptake and tissue penetration of nanomaterials.[10–13] In this study, the relationship between the surface chemistry and the penetration ability of Au NRs was investigated. We synthesized Au NRs with three different polymer coatings: cetyltrimethylammonium bromide (CTAB), polystyrene sulfonate (PSS) and poly (diallyldimethylammonium chloride) (PDDAC). All Au NRs have an aspect ratio of 4, while the LSPR maximum

†Electronic Supplementary Information (ESI) available: [Materials and methods section]. See DOI: 10.1039/b000000x/

*Address correspondence to liangxj@nanoctr.cn or wuxc@nanoctr.cn.
⊥These authors contributed equally to this work.

wavelength is 808 nm, which is the optimized wavelength for NIR thermal therapy. Dark-field (DF) imaging is commonly used for *in vitro* imaging of the Au NRs;[1, 14] however, the concentration of Au NRs near the solid tumor tissue is difficult to measure, and the solid tumor tissue is relatively large and complex. Therefore, it is difficult to observe the Au NRs distribution in the solid tumor using this technique. Hence, we employed a multicellular tumor spheroid (MCTS) as a model to study the Au NRs distribution. The MCTS is similar to solid tumor tissues in morphology, structure, function and gene expression,[15–19] but they are smaller and easier to establish. The interactions between the cells and their extracellular matrix in 3D cell culture enable them to maintain the unique features of tissues, especially the adherent cell junctions. We could obtain a visual proof of the Au NRs distribution through the MCTSs sections. The concentration of the Au NRs is adjustable and can be controlled to be much higher than in animal test. Thus, in comparison to *in vivo* test, the only factor that determines the penetration of the Au NRs is the difference in surface coating. Hence, MCTS is an ideal model for Au NRs penetration study. We predicted that different surface charges would affect the penetration and retention of the nanoparticles in tumors, resulting in different thermal therapeutic benefits.

Three types of Au NRs were synthesized following the protocol described in the methods section. The mean size of the Au NRs was 55 × 14 (length × diameter/nm), which was measured and statistically analyzed according to the TEM images. The UV-Vis-NIR absorption spectra demonstrated that maximum absorption peaks were close to 808 nm, which was in the NIR region. The soft tissue has low absorption in this region and laser penetration depth would be maximized.[6] Zeta-potential results showed that the PDDAC-coated Au NRs and the CTAB-coated Au NRs were positively charged, whereas the PSS-coated Au NRs were negatively charged (Fig. 1).

A series of environmental scanning electron microscopy (ESEM) images with different magnifications demonstrated the structure of the spheroids. The MCF-7 cells formed tightly packed round spheroids (Fig. 2A). The surface cells of the MCTSs were similar to in vivo tumor tissues but showed different morphologies compared to the monolayer cells. The cells in the MCTSs appeared crowded, compact and had an irregular spindle shape; while monolayer cells were more stretched.

Transmission electron microscopy (TEM) was performed to observe the cells outside and inside the MCTSs. The representative images are shown in Fig. 2B, and the nucleus shape was still normal in the outer cells. In the inner cells, however, the nucleus swelled and became malformed. A large amount of protuberances and invaginations occurred, which indicated bad cell viability. It has been reported that the proliferating and the non-proliferating tumor cell nuclei vary in shape, and tumor cells with low proliferative activity has a tendency towards a more irregular nuclear shape.[20] The outer and inner regions of the cylindroids have been shown to contain viable and apoptotic microenvironments, respectively.[21] The cells in the periphery were predominantly proliferating, while the cells in the center were mostly apoptotic and necrotic. This suggested that the radial organization mimics the distribution of cells around blood vessels in tumors in vivo. The outer region of the spheroid corresponded to the tumor tissue near the blood supply where cells can proliferate in the presence of sufficient oxygen and nutrients. The inner region of the spheroid was similar to the tumor tissue that was far away from the blood supply, where cells also grow with decreased oxygen and nutrient level.[22, 23] The cells in the inner region of the MCTS may be more vulnerable to thethermal therapeutic treatment. Therefore, spheroids were selected as a suitable model for evaluating the relationship between the penetration behavior of the Au NRs in tumor tissue and the thermal therapeutic efficacy.

The viability of the MCTSs treated with 150 pM Au NRs with different surface modifications for 24 h was assessed by acid phosphatase (APH) assay. Conventional cell viability assays need to digest the MCTSs in order to disperse cells before the assays. This step would damage cells and cause inaccuracy in the results. Hence, the APH assay was employed to avoid the disadvantages. This assay could be run without any pretreatment of the MCTSs and is more accurate in reflecting the cellular viability in the 3D cell culture model.[24, 25] As is shown in Figure 3A, the viability of the MCTSs was not affected significantly after 24 h of Au NRs treatment in different groups. Thus, the following experiments were conducted with 24 h Au NRs treatment to rule out the impact of cellular toxicity on the thermal therapy test result.

A quantitative, inductively coupled plasma mass spectrometry (ICP-MS) measurement was conducted to estimate the amount of Au NRs internalized by the spheroids. The ICP-MS results showed that PDDAC-coated Au NRs had the greatest amount of retention (Fig. 3B). It has been reported that in a monolayer cell culture, the PDDAC-coated Au NRs had the greatest cellular uptake amount, while the PSS-coated Au NRs had the least cellular uptake amount. The uptake dosage of the PDDAC-coated Au NRs was more than 16-fold compared with the CTAB-coated Au NRs and 30-fold compared with the PSS-coated Au NRs.[12] The tendency of Au NRs uptake in MCTSs is consistent with that of a monolayer cell culture; however, the difference is not that obvious. The number of Au NRs per spheroid treated with the PDDAC-coated Au NRs was only twice that of the PSS-coated Au NRs treated spheroids. The difference in the uptake of Au NRs between the PDDAC-coated and the CTAB-coated Au NRs treated groups was minimal. In a monolayer cell culture, cationic surface coatings will enhance the uptake of nanoparticles greatly.[26] While in MCTSs, this kind of surface coatings had effect only on the surface cells. Penetration is another key factor which is only present in MCTSs. Consequently, the results obtained in different cell culture models varied.

Thermal therapy is one of the major applications of Au NRs in cancer treatment; therefore, the bio-distribution of the Au NRs in tumor tissue would affect the therapeutic efficiency. The MCTSs were radiated under the NIR laser for 4 min after incubation with Au NRs for 24 h. The thermal therapy efficiency of each kind of Au NRs is shown in Fig. 3C and calculated according to the following formula:

$$\text{Thermal therapy efficiency} = \text{Viability loss} / \text{the Number of Au NRs per MCTS}$$

After laser radiation, the Au NR-treated MCTSs suffered great viability loss. The thermal therapy efficiency of the PSS-coated Au NRs was the highest, followed by the PDDAC-coated Au NRs. The CTAB-coated Au NRs had the lowest efficiency, which was less than 40 % of that of the PSS-coated Au NRs.

Hematoxylin-eosin (HE) staining was employed to observe the morphological change of MCTSs after thermal therapy. The HE staining result showed that radiation rarely had any effect on the control group, while the MCTSs treated with Au NRs showed a variety of structural changes. In the PSS-coated Au NRs group, a mass of inner cells were killed, and the skeleton was destroyed; hence, cavities appeared, the structure became loose, and the shape became irregular. The damage of inner cells was not obvious in the other two Au NRs treated groups, and cavities could only be seen at the border of the MCTSs (Fig. 3D).

To show the distribution of Au NRs in the MCTSs directly, DF microscopy was used to examine the penetration of Au NRs in the tumor spheroids. The DF microscope illuminated the samples with oblique beam and collected the reflected and scattered light for imaging.

Some metal materials, such as Au NRs, exhibit better reflecting property. Therefore, the interference of the dye used in HE staining can be excluded. In the sections of the PDDAC-coated Au NRs and the CTAB-coated Au NRs treated MCTSs, the reflected light of the Au NRs was around the spheroids (Figure 4b and 4f), which demonstrates that most of the Au NRs were distributed in the outer region of the MCTSs. The bright spots (Figure 4d) in the inner region of the MCTSs were Au NRs, which penetrated into the MCTSs. The DF images showed that the PSS-coated Au NRs can penetrate into the MCTSs and reach the inner regions of the cylindroids, while the other two Au NRs were distributed outside. The Au NRs used in the experiments were suspended in complete medium; therefore, they would interact with serum proteins. For physiological conditions, most serum proteins show slightly anionic property. For monolayer cells, the proteins would be adsorbed to the Au NRs, mediating their cellular uptake.[27, 28] Because serum proteins are diverse, the Au NR probably contained a variety of serum proteins nonspecifically adsorbed onto its surface. The PDDAC and the CTAB were cationic polymers, thus they would adsorb more proteins with negative charges. To support this assumption, the zeta potentials of three Au NRs were measured after incubation with serum containing medium for 24 hours. The PDDAC-coated and CTAB-coated Au NRs were found to be negatively charged after incubation, while the PSS-coated Au NRs remained their negative charge (Fig. S1). The proteins adsorbed by the negatively charged PSS Au NRs would be different from those of the other two Au NRs, and the presence and amount of these proteins on the surface of nanoparticles would affect their interaction with MCTSs. The positively charged Au NRs adsorbed more proteins on their surface and increased more in size compared with the negatively charged Au NRs and this dictates the penetration behavior of Au NRs into the spheroids. Consequently, the PSS-coated Au NRs had better penetration ability and were more homogeneously distributed in the spheroids, whereas the cationic polymer-coated Au NRs were distributed in the outer region or adsorbed on the surface of the spheroids. During radiation treatment, in the PSS-coated Au NRs treated group, the inner cells around the Au NRs were killed, and the compact structures were broken. The PDDAC or the CTAB-coated Au NRs were located or adhered to the border of the MCTSs; therefore only parts of the MCTSs were destroyed by hyperthermia. Consequently, the thermal therapy efficiency was limited despite the higher amount of Au NRs per MCTS.

It has been reported that positively charged nanoparticles improve the delivery of the payloads to the cells, whereas the negatively charged nanoparticles diffuse more rapidly, thereby delivering drugs deeper into tissues.[29] In this study, a MCF-7 multicellular tumor spheroid, which mimicked the distribution of the cells around the blood vessels in tumor tissue *in vivo*, was used for the thermal therapeutic evaluation of Au NRs with different surface coatings. The cells in the outer region of the spheroid corresponded to the tumor tissue near the blood supply having sufficient oxygen and nutrients, while the cells in the inner region of the spheroid were similar to the tumor tissue far away from the blood supply with decreased oxygen and nutrients. Therefore, the cells in the inner region of the MCTS may be more vulnerable to the thermal therapeutic treatment.

After the laser radiation, the APH assay proved that in comparison to the other two cationic polyelectrolyte-coated Au NRs, the PSS-coated Au NRs had the highest hyperthermia efficacy. In the PSS group, the compact structure of the MCTSs was broken by the Au NRs thermal therapy, and sections of the MCTSs appeared to be cracked. The DF images indicated an optimized spheroid distribution of the Au NRs in hyperthermia obtained by the negatively charged PSS Au NRs.

In conclusion, our results showed that surface charge can be used to control tissue penetration and thermal therapeutic efficacy. We believe that a relationship possibly exists between the adsorption of protein on the surface of Au NRs and their tumor spheroid

penetration efficiency. The difference in thermal therapy efficacy was due to the effective heat generated by the Au NRs with different surface coatings, which is affected by different Au NRs distribution patterns in the tumor. This conclusion may help guide the design of the surface chemistry of Au NRs for tailoring the thermal therapy.

Supplementary Material

Refer to Web version on PubMed Central for supplementary material.

Acknowledgments

This work was supported by grants from the Chinese Natural Science Foundation project (No.30970784), National Key Basic Research Program of China (2009CB930200), Chinese Academy of Sciences (CAS) “Hundred Talents Program” (07165111ZX) and CAS Knowledge Innovation Program. This work was also supported in part by NIH/NCRR/RCMI 2G12RR003048 and USAMRMC W81XWH-05-1-0291 grants.

Notes and references

1. Huang X, El-Sayed IH, Qian W, El-Sayed MA. J Am Chem Soc. 2006; 128:2115–2120. [PubMed: 16464114]
2. Bonoiu AC, Mahajan SD, Ding H, Roy I, Yong KT, Kumar R, Hu R, Bergey EJ, Schwartz SA, Prasad PN. Proc Natl Acad Sci U S A. 2009; 106:5546–5550. [PubMed: 19307583]
3. Von Maltzahn G, Park JH, Agrawal A, Bandaru NK, Das SK, Sailor MJ, Bhatia SN. Cancer Res. 2009; 69:3892–3900. [PubMed: 19366797]
4. Weissleder R. Nat Biotechnol. 2001; 19:316–317. [PubMed: 11283581]
5. Dickerson EB, Dreaden EC, Huang X, El-Sayed IH, Chu H, Pushpanketh S, McDonald JF, El-Sayed MA. Cancer Lett. 2008; 269:57–66. [PubMed: 18541363]
6. Xia Y, Li W, Cobley CM, Chen J, Xia X, Zhang Q, Yang M, Cho EC, Brown PK. Acc Chem Res. 2011; 44:914–924. [PubMed: 21528889]
7. Jain PK, Huang X, El-Sayed IH, El-Sayed MA. Acc Chem Res. 2008; 41:1578–1586. [PubMed: 18447366]
8. Jain PK, Lee KS, El-Sayed IH, El-Sayed MA. J Phys Chem B. 2006; 110:7238–7248. [PubMed: 16599493]
9. Minchinton AI, Tannock IF. Nat Rev Cancer. 2006; 6:583–592. [PubMed: 16862189]
10. Verma A, Stellacci F. Small. 2010; 6:12–21. [PubMed: 19844908]
11. Jain RK, Stylianopoulos T. Nat Rev Clin Oncol. 2010; 7:653–664. [PubMed: 20838415]
12. Qiu Y, Liu Y, Wang L, Xu L, Bai R, Ji Y, Wu X, Zhao Y, Li Y, Chen C. Biomaterials. 2010; 31:7606–7619. [PubMed: 20656344]
13. Nel AE, Mädler L, Velegol D, Xia T, Hoek EMV, Somasundaran P, Klaessig F, Castranova V, Thompson M. Nat Mater. 2009; 8:543–557. [PubMed: 19525947]
14. Murphy CJ, Gole AM, Stone JW, Sisco PN, Alkilany AM, Goldsmith EC, Baxter SC. Acc Chem Res. 2008; 41:1721–1730. [PubMed: 18712884]
15. Huang K, Ma H, Liu J, Huo S, Kumar A, Wei T, Zhang X, Jin S, Gan Y, Wang PC. ACS Nano. 2012; 6:4483–4493. [PubMed: 22540892]
16. Pickl M, Ries C. Oncogene. 2008; 28:461–468. [PubMed: 18978815]
17. Hirschhaeuser F, Menne H, Dittfeld C, West J, Mueller-Klieser W, Kunz-Schughart LA. J Biotechnol. 2010; 148:3–15. [PubMed: 20097238]
18. Kleinman HK, Philp D, Hoffman MP. Curr Opin Biotechnol. 2003; 14:526–532. [PubMed: 14580584]
19. Ong S-M, Zhao Z, Arooz T, Zhao D, Zhang S, Du T, Wasser M, van Noort D, Yu H. Biomaterials. 2010; 31:1180–1190. [PubMed: 19889455]
20. Nafe R, Herminghaus S, Pilatus U, Hattingen E, Marquardt G, Schlote W, Lanfermann H, Zanella F. Neuropathology. 2004; 24:172–182. [PubMed: 15484695]

21. Freyer JP, Sutherland RM. Cancer Res. 1980; 40:3956–3965. [PubMed: 7471046]
22. Fischbach C, Chen R, Matsumoto T, Schmelzle T, Brugge JS, Polverini PJ, Mooney DJ. Nat Methods. 2007; 4:855–860. [PubMed: 17767164]
23. Byrne HM. Nat Rev Cancer. 2010; 10:221–230. [PubMed: 20179714]
24. Friedrich J, Seidel C, Ebner R, Kunz-Schughart LA. Nat Protoc. 2009; 4:309–324. [PubMed: 19214182]
25. Friedrich J, Eder W, Castaneda J, Doss M, Huber E, Ebner R, Kunz-Schughart LA. J Biomol Screen. 2007; 12:925–937. [PubMed: 17942785]
26. Cho EC, Xie J, Wurm PA, Xia Y. Nano Lett. 2009; 9:1080–1084. [PubMed: 19199477]
27. Alkilany AM, Nagaria PK, Hexel CR, Shaw TJ, Murphy CJ, Wyatt MD. Small. 2009; 5:701–708. [PubMed: 19226599]
28. Hauck TS, Ghazani AA, Chan WC. Small. 2008; 4:153–159. [PubMed: 18081130]
29. Kim B, Han G, Toley BJ, Kim C, Rotello VM, Forbes NS. Nat Nanotechnol. 2010; 5:465–472. [PubMed: 20383126]

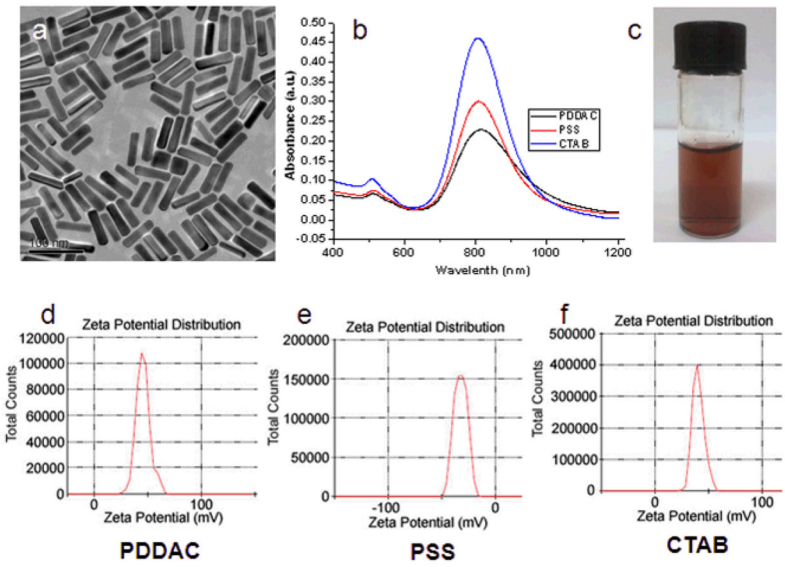

Fig. 1.

Characterization of Au NRs. (a) TEM image of the CTAB-coated Au NRs. (b) UV-Vis-NIR absorption spectra of PDDAC-coated Au NRs, PSS-coated Au NRs and CTAB-coated Au NRs. (c) Suspension of Au NRs. (d-f) Zeta potential distribution of PDDAC (d), PSS (e) and CTAB-coated Au NRs (f).

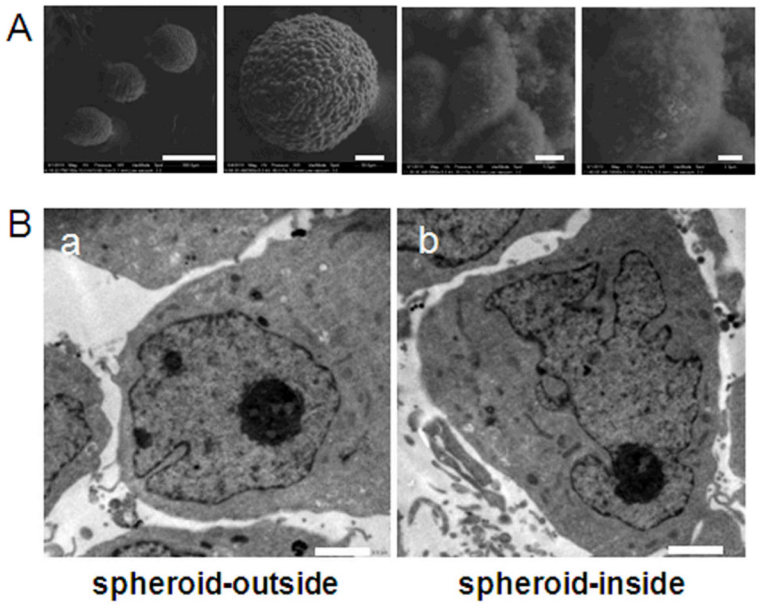

Fig. 2.

(A) ESEM images of MCF-7S spheroids after 7 days of culturing taken under a series of magnifications (Scale bar from left to right, 300 μm, 50 μm, 5 μm, 2 μm). (B) TEM images of cells on the outside (a) and inside (b) of the MCF-7 tumor spheroid (Scale bar, 2.0 μm).

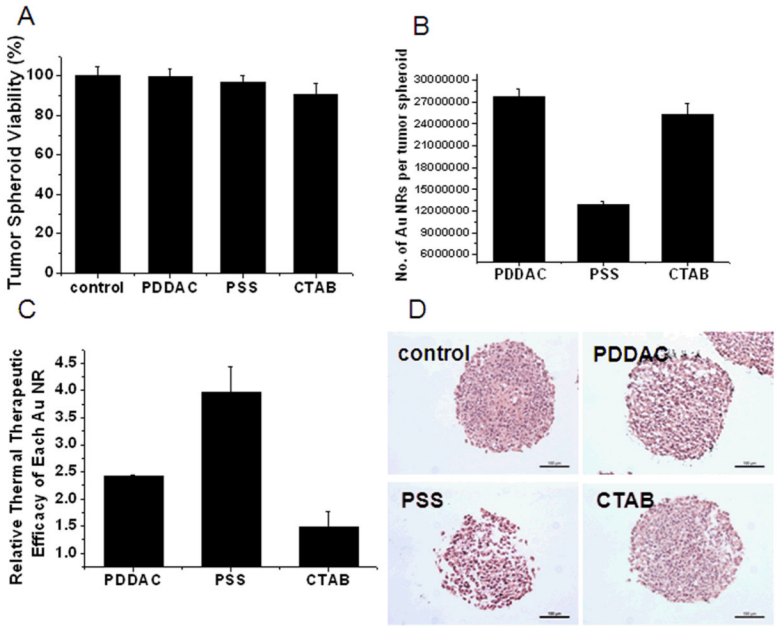

Fig. 3.

NIR thermal therapy effect. (A) Tumor spheroid viability after treatment with different Au NRs at 150 pM for 24 h. (B) The number of Au NRs per tumor spheroid after 24 h of treatment. (C) Thermal therapy efficiency of different Au NR calculated by the following formula: Thermal therapy efficiency = Viability loss/The number of Au NRs per MCTS. (D) HE staining. MCTSs were sectioned and stained after NIR laser radiation (Scale bar, 100 μm).

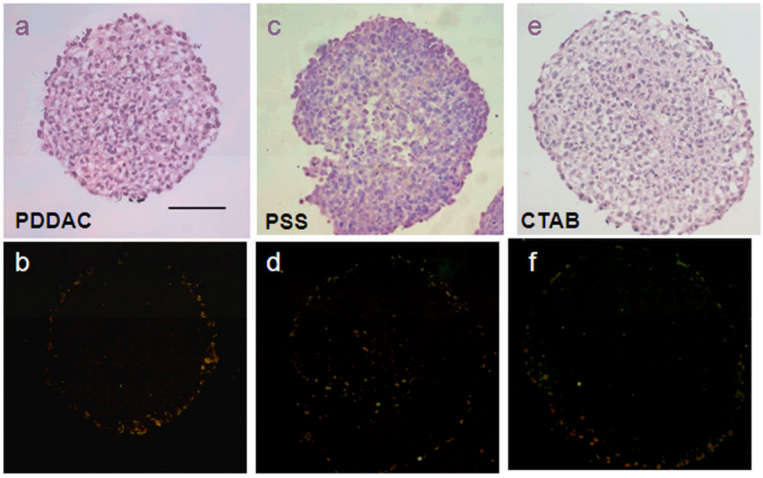

Fig. 4.

Distribution of Au NRs in MCTSs. HE staining of the tumor spheroid treated with different Au NRs for 24 h (a, c. e). DF images of tumor spheroid treated with different Au NRs for 24 h (b. d. f). The bright spots in the DF images represent for the existence of Au NRs. In b and f, Au NRs are distributed mainly outside. In d, Au NRs are distributed both outside and inside (Scale bar, 100 μm).